

THE INFLUENCE OF A CRACK NEIGHBORHOOD ON THE ELASTIC ENERGY OF A LOOP DISLOCATION

Angelo Gil Pezzino Rangel

Universidade Federal do Espírito Santo – Centro Tecnológico – Programa de Pós-Graduação em Engenharia Mecânica – Av. Fernando Ferrari s/n – Goiabeiras – Vitória (ES) – 29060-900
gilrang@npd.ufes.br

Berenice M. Gonzalez

Universidade Federal de Minas Gerais – Escola de Engenharia – Departamento de Metalurgia e de Materiais – R. Espírito Santo
berenice@demet.ufmg.br

Abstract. *A semi-analytic three-dimensional model was developed to calculate the elastic energy variation which appears as a result of the interaction of a dislocation loop within a monocrystalline material and a crack. Application was made to a FCC material where there exist a crack and one loop aiming (i) to establish the conditions for a loop nucleation to occur ahead of the crack front and (ii) to study the amplitude variations on the results produced by this interaction. Changes in crack propagation conditions (shielding and antishielding) due to the presence of the loop were determined based on the stress intensity factor calculations. An entirely three-dimensional formulation was used to account for the stored elastic energy variation due to the interaction. A computer program called DiFrac was setup based on the proposed formulation which simulates crack-dislocation loop interaction and to calculate the associated image-force. The computer program has also allowed determining nucleation conditions of a loop dislocation.*

Keywords. *crack-dislocation interaction, elastic energy, nucleation of dislocations, shielding and antishielding*

1. Introduction

Even under the action of small forces, the presence of stress concentrators may induce the appearance of dislocations within the lattice of a crystalline material. It is, thus, natural to expect the presence of dislocations near a crack. It has been experimentally observed (George & Michot, 1993, George *et al.*, 2001) that, for nearly perfect materials under critical temperatures, dislocation nucleation occurs right in front of a crack. In real cases, they assume the shape of a loop that is enlarged thanks to a competition between the work done by the applied external forces and the elastic energy stored in the region within the influence of the dislocation. The first is approximately proportional to the inside area of the loop, while the second can be regarded as proportional to the loop perimeter. The balanced energy variation leads to the maximum free energy of the crystal when the loop radius reaches a critical value. If this critical radius has its order of magnitude close to the one of the Burgers' vector, emission occurs spontaneously for very small energy levels and the dislocation can be thermally activated. However, calculations made for the emission of a loop dislocation in an infinite medium of a perfect material, such as silicon, have shown very large values for both the critical radius and the energy barrier. This indicates silicon is intrinsically fragile, its rupture being possible only by cleavage, contradicting the experimental findings. Is there a condition for which a brittle to ductile (BTD) transition occurs in the material thus allowing it to develop loop dislocations and undergo a small plasticity, even being this material of an intrinsically fragile nature? How does the free surface of a crack interfere in the free energy of the crystal and reduce the energy barrier?

These are questions that persist to remain unanswered when the three-dimensionality of the problem is considered. Rice & Thomson (1974) have made the first attempts to solve the issue, but, as noted by Schöeck (1991), apart from making a rather thorough investigation on the subject, the problem they treated fell back to two dimensions. Oliveira (1994) formulated the first three-dimensional equations that led to a semi-analytic determination of the stress intensity factors induced on the crack by the presence of a loop dislocation. The loop rested on a general plane and touched the edge of the crack in just one point. Based on the same formulation, Rangel *et al.* (2001) presented a broader solution scheme which took advantage of some characteristics of the problem which are inherited from the resulting shape of the stress field induced by the loop. This approach allowed a more rational calculation of the energy variation due to the proximity of the loop and the crack's free surface (Rangel, 2002).

While addressing the questions posed above, the results presented herein intend to contribute to the solution of the problem by: (i) showing the main procedural steps used by Rangel (2002) to calculate the free energy variation as a loop approaches the edge of a crack in any angle n in an almost perfect crystal; (ii) analyzing the conditions for the nucleation of a loop in the region ahead of a crack; and (iii) evaluating the consequences of amplitude variations on the crack-loop dislocation interaction.

2. The energy variation in the interaction of a crack and a loop dislocation

Following Rangel (2002), the basic equations used to calculate the free energy variation in the interaction of a crack and a loop dislocation are presented with their solution.

2.1. The stress field and its shape

Considering \mathbf{b} the Burgers' vector of a loop dislocation with radius $\rho' = N |\mathbf{b}| = N b$, where $N \in \mathbb{I}$, the stress at a point M, distant R from the loop's center C, in a material with shear stress μ , can be found in Hirth & Lothe (1968) as

$$\begin{aligned} \boldsymbol{\sigma}'' = \boldsymbol{\sigma}''_{ij} \mathbf{g}''_i \otimes \mathbf{g}''_j = \frac{\mu}{8\pi} \left\{ \oint_C b_m \varepsilon_{kmi} \frac{\partial}{\partial x_k} (\nabla''^2 R) dx_j'' - \oint_C b_m \varepsilon_{kmj} \frac{\partial}{\partial x_k} (\nabla''^2 R) dx_i'' + \right. \\ \left. - \frac{2}{(1-\nu)} \oint_C b_m \varepsilon_{kmn} \left[\frac{\partial^3 R}{\partial x_k \partial x_i \partial x_j} - \delta_{ij} \frac{\partial}{\partial x_k} (\nabla''^2 R) \right] dx_n'' \right\} \mathbf{g}''_i \otimes \mathbf{g}''_j. \end{aligned} \quad (1)$$

Rangel *et al.* (2002) rewrote the stress components σ''_{ij} in their nondimensional form as

$$\begin{aligned} \sigma'_{ij} = \frac{\sigma''_{ij}}{\mu} = \frac{1}{8\pi} \left\{ \oint_C l_m \varepsilon_{kmi} \frac{\partial}{\partial \xi_k} (\nabla''^2 P) d\xi_j'' - \oint_C l_m \varepsilon_{kmj} \frac{\partial}{\partial \xi_k} (\nabla''^2 P) d\xi_i'' + \right. \\ \left. - \frac{2}{(1-\nu)} \oint_C l_m \varepsilon_{kmn} \left[\frac{\partial^3 P}{\partial \xi_k \partial \xi_i \partial \xi_j} - \delta_{ij} \frac{\partial}{\partial \xi_k} (\nabla''^2 P) \right] d\xi_n'' \right\}, \end{aligned} \quad (2)$$

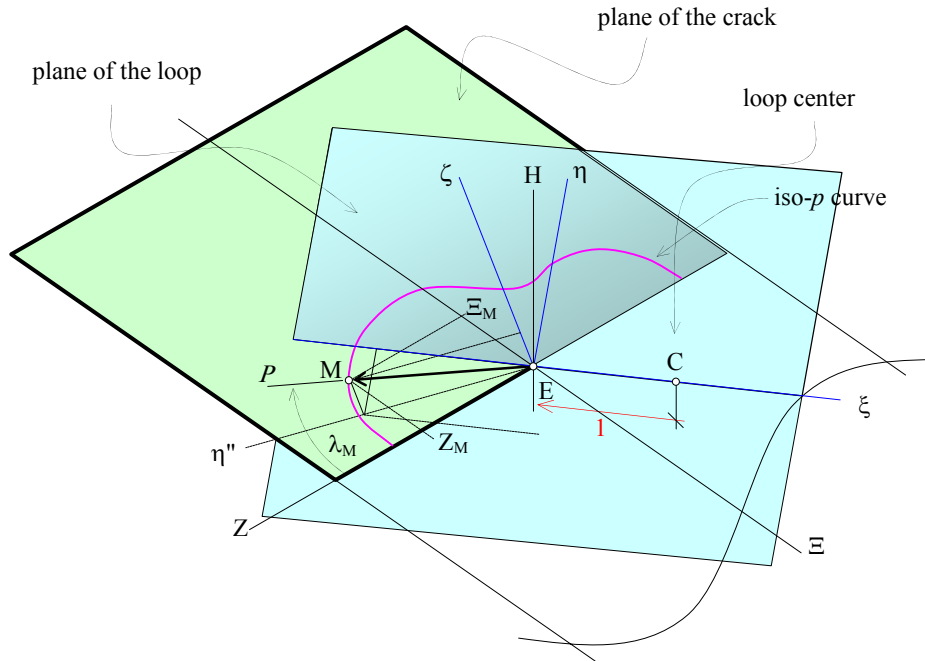


Figure 1. Nondimensional coordinates of point M over the crack plane, where one iso- p curve can be seen.

where $\xi_i = x_i / \rho'$, $P = R / \rho'$. Each component in Eq. (2) can be integrated by using elliptic functions of first and second kinds, $\mathcal{K}(p)$ and $\mathcal{E}(p)$, respectively (Abramowitz & Stegun, 1965). The parameter p is calculated as a function of the relative position of point M with respect to C [see Fig. (1)]. It also plays a very strong role in the shape of the stress distribution, suggesting a mesh can be created based on the variation of p , which is done in Fig. (2). In fact, this strong dependency of stresses and p has suggested the use of the iso- p curves shown in Fig. (2) to generate the mesh, thus leading to a much improved computational solution of the problem. A thorough explanation of the procedures can be found in Rangel *et al.* (2001) and Rangel (2002).

2.2. The stress intensity factors – K_I , K_{II} and K_{III}

The three stress intensity factors can be calculated when the loop touches the edge of the crack by

$$\mathbf{K}_J = \frac{1}{\rho'} \begin{Bmatrix} K_{II}(\Xi_0, Z_0) \\ K_I(\Xi_0, Z_0) \\ K_{III}(\Xi_0, Z_0) \end{Bmatrix} = \frac{\sqrt{2N}}{\pi^2} \int_{-\infty}^0 \int_{-\infty}^{+\infty} \mathbf{m} \mathbf{G}(\Xi_0, Z_0) \boldsymbol{\tau}(\Xi, Z) dZ d\Xi, \quad (3)$$

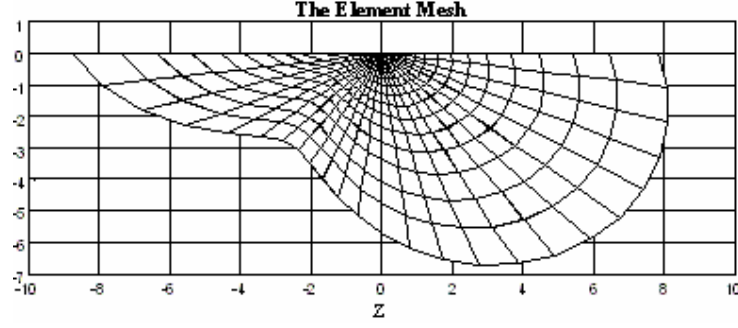


Figure 2. The element mesh based on parameter p .

or, approximately, by

$$\mathbf{K}_J = \frac{\sqrt{2} N}{\pi^2} \sum_{e=1}^L \sum_{k=1}^L \mathbf{m} \mathbf{G}_k(Z_0) \boldsymbol{\tau}_k(\Xi_M, Z_M) w_k(\Xi_M, Z_M) A_k, \quad (4)$$

where

$$\mathbf{m} = \begin{bmatrix} 1 & 0 & 0 & f & 0 \\ 0 & 1 & 0 & 0 & 0 \\ 0 & 0 & 1 & 0 & f \end{bmatrix}, \quad \text{with } f = \frac{2\nu}{(2 - \nu)}, \quad (5)$$

$$\mathbf{G}(\Xi_0, Z_0) = \begin{bmatrix} G_1 & 0 & 0 \\ 0 & G_1 & 0 \\ 0 & G_3 & -G_2 \\ 0 & G_2 & G_3 \\ 0 & 0 & G_1 \end{bmatrix}, \quad (6)$$

$G_1(\Xi, Z)$, $G_2(\Xi, Z)$ and $G_3(\Xi, Z)$ being weighting functions expressed in terms of nondimensional coordinates, as put by Rangel (2002). Also, the stress components needed in Eq. (4), $\boldsymbol{\tau}$, are only those related to the plane of the crack and represented in the coordinates defining this plane, namely τ_{HH} , $\tau_{H\Xi}$ and τ_{HZ} .

The mesh seen in Fig. (2) was obtained as a function of the stress distribution, since the iso- p curves are actually related to stresses and vice-versa. As a result of this dependency, for each specific problem the mesh is automatically generated.

When compared, both Eqs. (3) and (4) reveal the main advantage of considering this approach, since the integration limits in the later do not go beyond the meshed area. This is a very important feature which is achieved by this formulation, since the integrals in Eq. (4) will later be performed several times, at least once for each point along the edge of the crack, in order to bring up detailed stress intensity factor variations.

2.3. Changes in the stress intensity factors as the loop approaches de edge of the crack

The free surface of the crack offers an opportunity of energy relaxation to the loop. As the loop is considered at points approaching that free surface its stress field plays an increasing role in the interaction, meaning the stress intensity factors induced by the loop also increase. However, it is very hard to determine at which point along this “path” to the free surface this role becomes significant enough to interfere in the behavior of the crack. In other words, where around the crack does the loop begin to affect the crack behavior? It seems to be more reasonable, from the computational point of view, to consider the loop as “walking” this virtual path in the opposite sense, which is starting at a point where it touches the crack’s edge and then getting apart from it up to a point where it no longer has an appreciable influence on the crack. This is seen in Fig. (3).

Equations were developed by Rangel (2002) to calculate the stress intensity factor variations due to this “getting away path” of the loop. The greatest difficulty in the task was to keep the original mesh untouched and use it to calculate the new stress intensity factor. A hint of this technique is shown in Fig. (4), where the virtual displacement $\boldsymbol{\delta}$ is decomposed in direction Ξ and Z as

$$\boldsymbol{\delta} = \delta_{\Xi} \mathbf{g}_{\Xi} + \delta_Z \mathbf{g}_Z. \quad (7)$$

This procedure has a small drawback for it changes the crack edge from a straight line into a zig-zag, which is still acceptable, provided the size of the elements remains within a reasonable range.

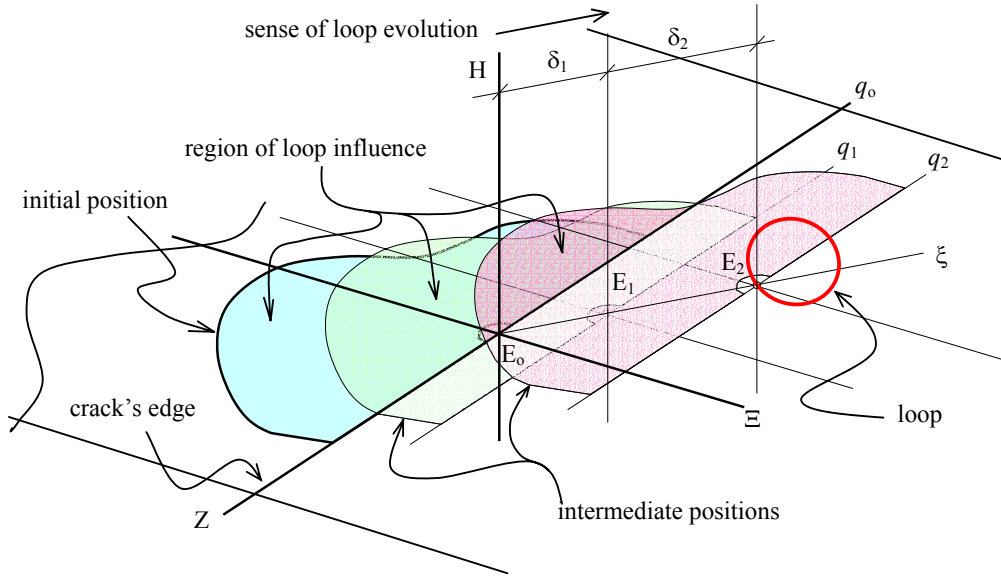


Figure 3. Evolution of the region of influence of the loop where stresses are capable of affecting the crack behavior. One notes that only the part of that region overlapping the crack free surface is considered in the integration of the stress intensity factor equations.

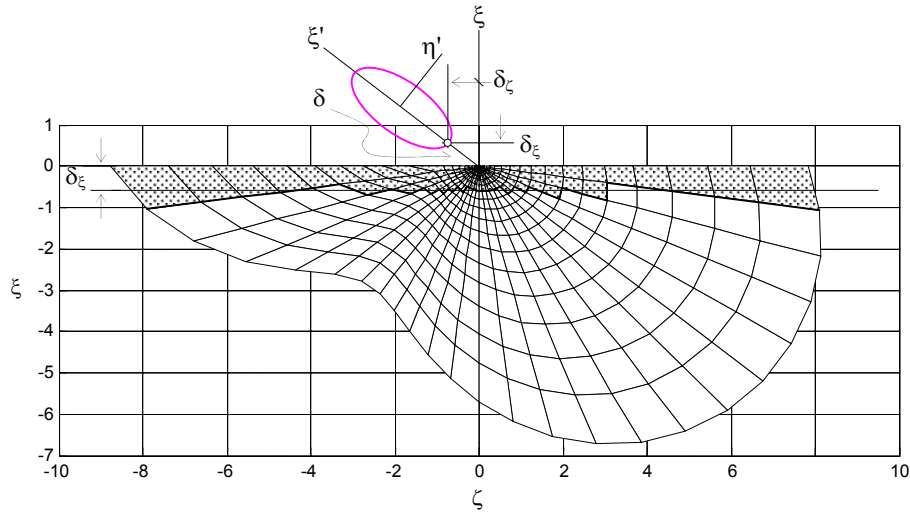


Figure 4. The mesh for integrating the stress intensity factor equations: shaded elements are taken away from the region of integration. Stress intensity factors are then calculated for the resulting area (unshaded elements).

2.4. The image force and its relation to the Irwin's equation

Once all stress intensity factors induced by the loop have been determined, Irwin's equation can now be calculated. In three-dimensional problems, this is

$$\mathcal{G} = -[(K_I)_d^2 / H_I + (K_{II})_d^2 / H_{II} + (K_{III})_d^2 / H_{III}] = -\frac{\partial \Pi_p}{\partial A}, \quad (8)$$

where H_I , H_{II} and H_{III} are elastic constants in their nondimensional form, given in Tab. (1), Π_p is the potential energy and A is the crack free surface. The image force can be obtained for each position of the loop along its virtual path towards the crack free surface by

$$\frac{\partial \mathbb{E}}{\partial r} = f_1, \quad (9)$$

\mathbb{E} being the elastic energy due to the presence of the loop and r the coordinate measured along the smaller straight line lying in the loop plane and linking the loop center and the crack edge, seen in Fig. (5).

Table 1. Nondimensional elastic constants H_j for the calculation of the image force.

State	Opening mode		
	I	II	III
Plane stress	$2 / (1 - \nu)$	$2 / (1 - \nu)$	2
Plane deformation	$2 (1 + \nu)$	$2 (1 + \nu)$	$2 (1 + \nu)(1 - \nu)$

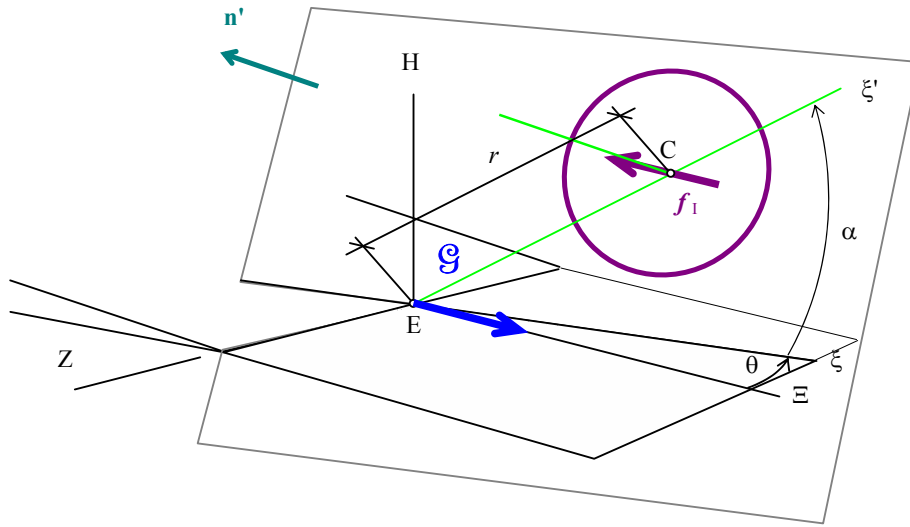


Figure 5. Forces acting on the loop and on the crack: f_1 – image force; g – extension force, respectively.

When applying the second of Newton's Laws to Eqs. (8) and (9), one is led to

$$f_1 = -g. \quad (10)$$

2.5. The energy balance

The relaxation energy corresponds to the reduction in the elastic energy stored by the presence of the loop. It is due to the proximity of the crack free surface. As the distance between loop and free surface diminishes, the energy relaxation becomes stronger, thus reducing the elastic energy of the loop. This energy variation is equivalent to the virtual work done by the image force through the virtual path of the loop, along $\xi' \equiv r$, which can be expressed as

$$\mathbb{W}_I = \int_0^{+\infty} f_1 dr = - \int_0^{+\infty} \frac{K_d^2}{H} dr = -\mathbb{E}_r(r). \quad (11)$$

The total elastic energy due of the system is

$$\mathbb{E}_T = \mathbb{E}^\infty - \mathbb{E}_r(r), \quad (12)$$

for which \mathbb{E}^∞ is the elastic energy in an infinite medium and $\mathbb{E}_r(r)$ the elastic energy due to the internal loading represented by the loop. The work done by the external loading can be approximated by

$$\mathbb{W}_D = \eta(\chi) K_I b \rho^{3/2}, \quad (13)$$

where $\eta(\chi)$ is a function of the crystal lattice that is approximated by a fifth order polynomial (Michot, 1982). Gibbs' energy associated with the problem can be obtained through

$$\Delta G = \mathbb{E}_T - \mathbb{W}_D = \mathbb{E}^\infty - \mathbb{E}_d - \mathbb{W}_D, \quad (14)$$

or, in nondimensional form,

$$\Delta G / \mu b^3 = \mathbb{E}^\infty / \mu b^3 - \mathbb{E}_d / \mu b^3 - \mathbb{W}_D / \mu b^3. \quad (15)$$

Figure (6) shows a qualitative plot of Gibbs' energy for the interaction of a loop dislocation and a crack. As it was stated earlier, the energy barrier is quite high and the critical loop radius quite large for an almost perfect material such as silicon.

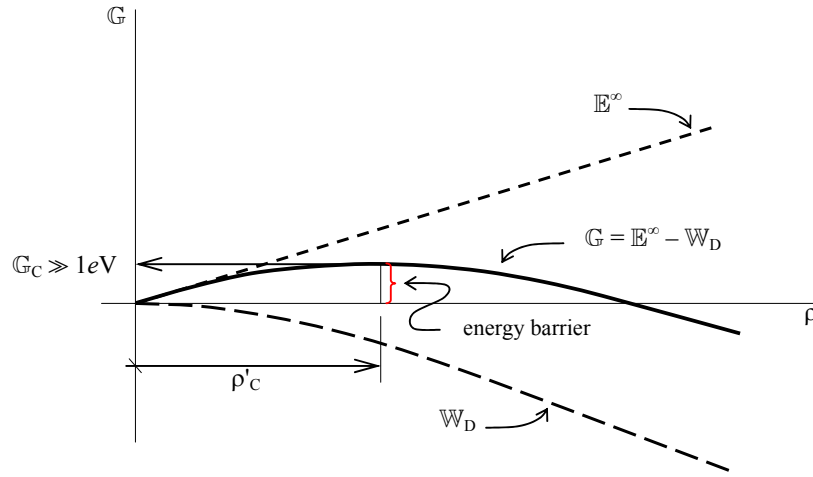


Figure 6. Gibbs' free energy associated with a loop dislocation. One can see the energy barrier that must be surpassed in order to nucleate a loop with radius ρ'_c .

2.6. Results for silicon

The procedure above was set up for a model based on silicon. Equations were solved for three lattice configurations as proposed by Michot (1982) under several relative positions of loop and crack. A computer program named DiFrac was conceived to be as flexible as possible, so all actual combinations of configuration, Burgers' vector, loop radius and angle of emission can be used as input in order to be analyzed. Some of these combinations are shown here for illustrating its capabilities.

Using configuration GAMMA (Rangel, 2002), for a loop radius $\rho' = 50 b$, with angle of emission $\alpha = 0$, results can be compared to experimental findings presented by Scandian *et al.* (1998) and Scandian (2000). Figure (7) shows the energy variation calculated for Burgers' vectors $\mathbf{b} = [1\ 0\ 1]$ (-1 1 1) and $\mathbf{b} = [0\ -1\ 1]$ (1 1 1). One sees that the second Burgers' vector stores more energy than the first one in this configuration. Since it demands less energy from externally applied loading in order to be activated, the second Burgers' vector will always show up before the first one. This fact has been experimentally verified by Scandian (2000), even when all conditions favoring the appearance of the first vector were imposed.

Keeping the same radius for the loop and taking, now, the BETA configuration, for $\mathbf{b} = [-1\ -1\ 0]$ (-1 -1 1), the angle of emission (or angle of incidence) α is let to vary from $-\pi/2$ to $+\pi/2$. The change in the elastic energy for several positions of α is given in Fig. (8).

2.7. Shielding and antishielding

Let a body with a crack to be loaded by externally applied forces, leading to a state of stresses at a point around the crack defined by σ_A . Assuming a loop dislocation is emitted within the material on a generic plane close enough to the crack edge, so that it generates a stress state σ_d . Using the principle of superposition, $\sigma_e = \sigma_A + \sigma_d$ is the total stress state at a point located in that region. The induced stress intensity factor can also be assumed as

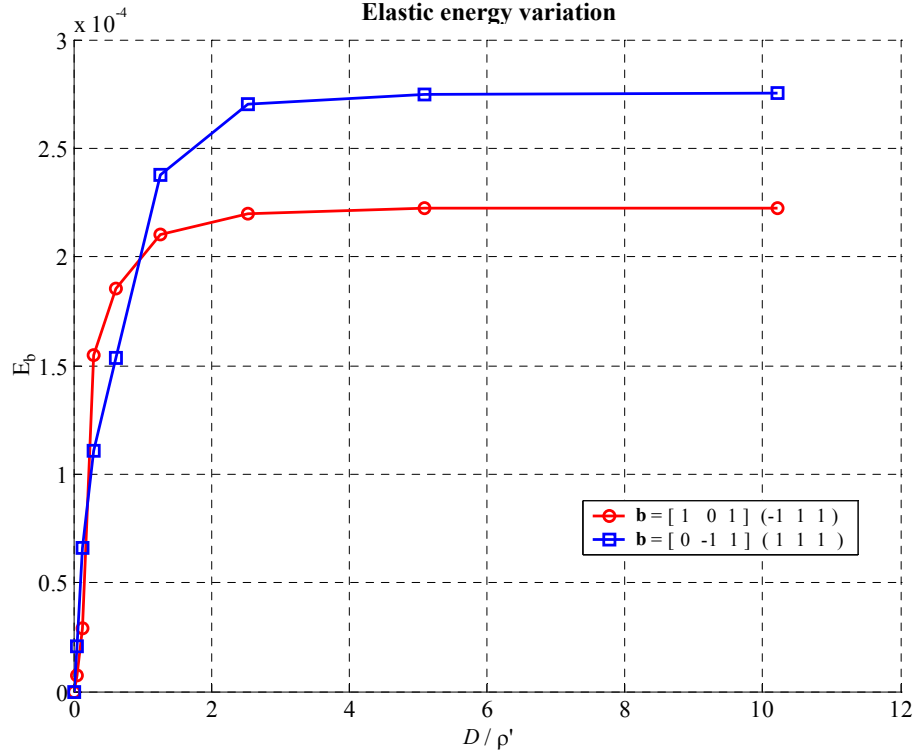


Figure 7. Stored elastic energy for different points of the loop dislocation along direction ξ' .

$$K_e = K_A + K_d. \quad (16)$$

The crack extension force given by Eq. (8) can be expressed as

$$\mathcal{G} = \frac{K_e^2}{H} = \frac{(K_A + K_d)^2}{H} = \frac{K_A^2}{H} + \frac{K_d^2}{H} + 2 \frac{K_A \cdot K_d}{H}. \quad (17)$$

By looking at Eq. (17) one can readily verify that the intensity and the sign of \mathcal{G} will depend only on the sign of the product $K_A \cdot K_d$. Hence, if $K_A \cdot K_d > 0$, the crack extension force will be greater than the extension force caused by adding the two effects, *i. e.*, $\mathcal{G}_A + \mathcal{G}_d$. On the other hand, if $K_A \cdot K_d < 0$, the extension force will be smaller than the sum of the effects. In the first case, there occurs a phenomenon called antishielding, indicating that crack propagation is favored. The second case is called shielding and the loop plays the role of an inhibitor of crack propagation.

2.8. The energy barrier

Rangel (2002), using the example shown in Fig. (9), calculated the Gibbs' free energy through Eq. (15). The conclusion was that the term due to the loop, $\mathbb{E}_d / \mu b^3$, is much smaller than the term $\mathbb{E}^\infty / \mu b^3$, indicating the nearness of the crack free surface has negligible influence on the interaction. Experimentally, the temperature is held constant while external loading is applied very slowly. Loop dislocation emissions are identified to begin for $K_I \cong 0,25 K_{IC}$, where $K_{IC} \cong 1 \text{ MPa m}^{1/2}$ for monocrystalline silicon (Michot, 1989). This leads to critical nondimensional nucleation energy $\Delta G_c / \mu b^3$ of, approximately, 4.000 (equivalent to 108.000 eV for $\Delta G_c!$), corresponding to a critical nucleation radius $\rho_c' = 3.000b$, as shown in Fig. (9).

2.9. Discussion of the results

If a dislocation loop of radius ρ' with Burgers' vector \mathbf{b} lying on a plane \mathbf{n} is emitted following an orientation in the range $-\pi/2 < \alpha < +\pi/2$ for the three accepted lattice configuration arrangements, the procedure presented above can:

- (a) determine the evolution of stress intensity factors induced by the presence of the loop on the edge of the crack;

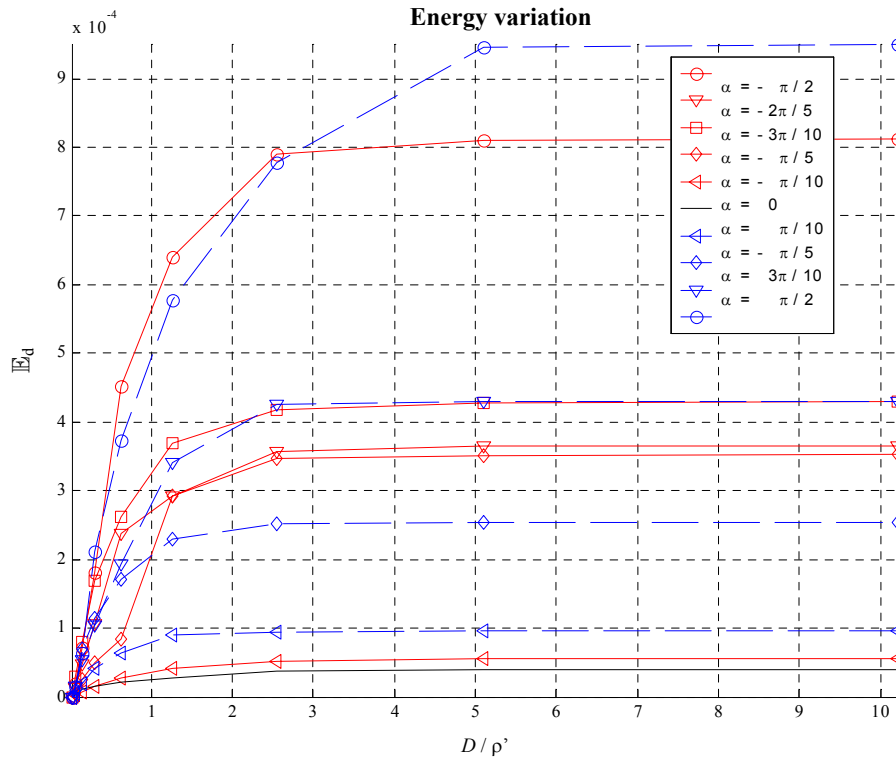


Figure 8. Elastic energy variation for different emission angles α and for loops away from the crack edge.

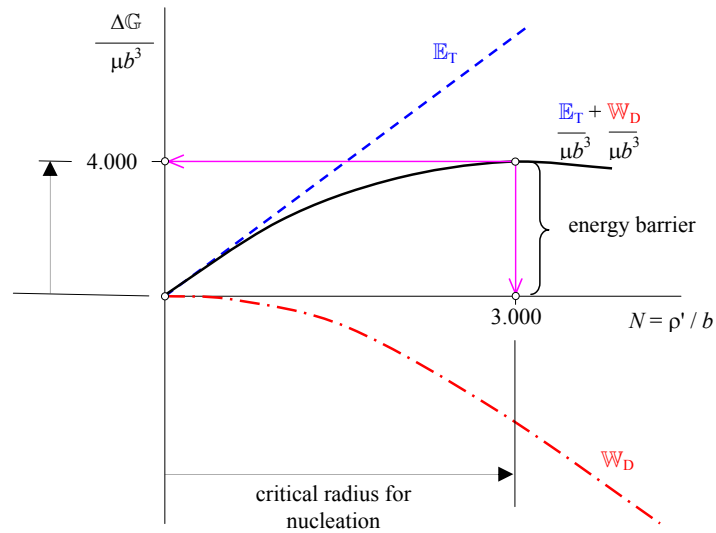


Figure 9. Schematic plot where one can see the energy barrier when a $0,25 K_{IC}$ external loading is applied to the body with a crack and a loop nearby at a constant temperature.

- (b) determine the region of influence of the loop over the crack edge;
- (c) calculate an average value for the stress intensity factors, such as

$$\langle K_J \rangle = \int_l^l \frac{K_J}{l_f - l_i} dZ, \quad (18)$$

- where one can observe that $\langle K_j \rangle$ can: *i*) change its sign with the angle of emission; *ii*) proportionally decrease as the distance between the loop and the crack increases; and *iii*) decreases with the increase in the loop radius;
- (d) calculate the crack extension force and, consequently, the image force component in the direction of the crack propagation;
 - (e) determine the same parameters for any relative position between loop and crack;
 - (f) calculate the work done along a virtual path and the increase of the energy as the loop gets away from the crack.

2.10. Conclusions

The nondimensional formulation of the equations of a three-dimensional interaction between a loop dislocation and a crack has made possible the determination of the nucleation energy of loop dislocations near a crack tip. This has been done for an almost perfect material with a well defined lattice. It has been observed a strong dependency on the nucleation conditions.

Carefully established integration schemes have led to quite accurate results, even when approximations are made in order to accelerate integration routines. The procedure can be extended to other types of crystal defects.

The calculations of the energy barrier have shown that there cannot be any spontaneous nucleation of loops ahead of a perfect crack edge. Embryonic loops already within the material lattice and the stress field induced by the external loading determine the planes where dislocation loops will develop, as well as their slip planes. In configuration BETA, loop dislocations are responsible for shielding the crack-tip.

3. Acknowledgement

The authors are indebted to Gérard Michot for very helpful discussions and insight on the subject. Also, to CAPES and Cia. Siderúrgica de Tubarão for supporting the work.

4. References

- Abramowitz, M. and Stegun, I.A., 1965, Handbook of Mathematical Functions, Dover Pub., NY, Sec. 17.
- George, A. and Michot, G. 1993, "Dislocation loops at crack tips: nucleation and growth – An experimental study in Silicon", *Mat. Sci. Eng.*, A164, pp. 118-134.
- George, A. *et alli*, 2001, "Viewpoint Set on: Dislocation mobility in Silicon", *Scrip. Mat.*, **45**, pp. 1233-1294.
- Hirth, J.H. and Lothe, J., 1982, Theory of Dislocations, 2nd ed., Krieger Pub., Malabar, Florida.
- Michot, G., 1982, Doctoral thesis presented to INPL, Nancy, France.
- Michot, G., 1989, "Fundamentals of Silicon fracture", in Crystal Properties and Preparation, vols. 17 & 18, Trans. Tech Publications, Switzerland, pp. 55-98.
- Oliveira, M.A.L., 1994, "Émission et développement de dislocations en tête de fissure dans le Silicium: analyse tridimensionnelle de l'interaction dislocation/fissure", Doctoral thesis presented to INPL – Nancy, France.
- Oliveira, M.A.L., Rangel, A.G.P. and Michot, G., 2001, "Plastic Relaxation at crack tips: Micro-mechanical analysis", *Mat. Trans. of the JIM*, vol. 42, pp. 20-27.
- Rangel, A.G.P., (2002), "Influência da vizinhança de uma trinca sobre a energia elástica de uma discordância em anel", Doctoral thesis presented to CPGEM, UFMG, Belo Horizonte, Brazil.
- Rangel, A.G.P., Gonzalez, B.M. and Helman, H., 2001, "The three-dimensional interaction of lattice defects and the propagation of cracks", XVI Congresso Brasileiro de Engenharia Mecânica, 25-30/nov, Uberlândia (MG) (publicação eletrônica em CD-ROM).
- Rice, J.R. and Thomson, R., 1974, "Ductile versus brittle behaviour of crystals", *Phil. Mag.*, pp. 29-73.
- Scandian, C., 2000, "Conditions d'émission et de multiplication des dislocations à l'extrémité d'une fissure: Application au cas du Silicium", Doctoral thesis presented to INPL – Nancy, France.
- Scandian, C., Azzouzi, H., Maloufi, N. and Michot, G., 1998, "Dislocation nucleation and multiplication at crack tips in Silicon", *Phys. Stat. Sol. (A)*, **171**, pp. 67-81.

5. Copyright Notice

The author is the only responsible for the printed material included in his paper.